RESEARCH ARTICLE

Preparation and anti-inflammatory analgesic effects of cannabidiol film-forming gel

Yanli Zhao, Linshuang Guo, Zihao Jiang, Xiaoyi Chen, Min Yuan, Liyuan Sui, Dajing Li, Xiaofan Wu, Zan Li*

School of Pharmacy, Jiamusi University, Jiamusi, Heilongjiang, China.

Received: April 22, 2026; **accepted:** July 25, 2026.

Pain commonly accompanies diverse pathological conditions and can substantially impair daily functioning and quality of life. This study developed a cannabidiol (CBD) film-forming gel as a topical analgesic and anti-inflammatory formulation to overcome the formulation challenges associated with the high lipophilicity and poor aqueous solubility of CBD. The formulation was optimized using single-factor experiments and an orthogonal design with carboxymethyl cellulose sodium as the gel matrix and polyvinylpyrrolidone as the film-forming agent. Analgesic activity was evaluated using the acetic acid-induced writhing test, while anti-inflammatory activity was assessed using xylene-induced ear swelling and egg white-induced paw swelling models in mice. Serum IL-4, IL-6, and TNF-α levels were measured by using enzyme-linked immunosorbent assay (ELISA), and preliminary safety was evaluated based on general condition, body weight, and major-organ indices. The optimized formulation contained 0.0019 g CBD per 10 g gel. The formulation appeared as a pale, milky-white, translucent liquid with a pH of 5.5 – 6.0 and a particle size of approximately 12.4 μm and exhibited good physical stability. CBD film-forming gel significantly reduced acetic acid-induced writhing with the high-dose group achieving a pain inhibition rate of 60.0%. It also inhibited xylene-induced ear swelling and showed a tendency to alleviate egg white-induced paw swelling. Histopathological examination indicated reduced tissue edema and inflammatory cell infiltration, particularly in the medium- and high-dose groups. Serum cytokine levels showed IL-4 level in the high-dose group was significantly elevated compared with the control group ($P < 0.001$). No obvious treatment-related abnormalities were observed. Overall, the formulation exhibited satisfactory physicochemical properties, marked analgesic activity, potential local anti-inflammatory effects, and a favorable preliminary safety profile.

Keywords: cannabidiol; film-forming gel; formulation optimization; quality evaluation; anti-inflammatory; analgesic.

***Corresponding author:** Zan Li, School of Pharmacy, Jiamusi University, Jiamusi, Heilongjiang 154007, China. Email: lizan4432@163.com.

Introduction

Pain and inflammation are common features of numerous diseases including arthritis, musculoskeletal disorders, and infections, and can substantially impair patients' quality of life [1, 2]. More than 20% of adults worldwide are estimated to experience chronic pain, resulting in considerable physical, psychological, and socioeconomic burdens [3, 4]. Current pharmacological treatments for pain and inflammation primarily include non-steroidal anti-inflammatory drugs (NSAIDs) and opioid analgesics [5, 6]. However, long-term NSAID use is associated with gastrointestinal injury, cardiovascular risk, and renal toxicity [7, 8], whereas opioids carry substantial risks of dependence, respiratory depression, and

tolerance [9, 10]. There remains a clear need for safer and more effective therapeutic strategies.

Cannabidiol (CBD) is a non-psychoactive phytocannabinoid derived from *Cannabis sativa* L. ($C_{21}H_{30}O_2$) that has attracted considerable scientific interest in recent years [11, 12]. Unlike Δ9-tetrahydrocannabinol (THC), CBD does not produce euphoric effects or activate the brain reward system and is generally considered to have a favorable safety profile [13]. Accumulating evidence suggests that CBD possesses a broad range of pharmacological activities. Its analgesic and anti-inflammatory effects have been linked to activation of cannabinoid receptor 2 and modulation of 5-hydroxytryptamine 1A receptors [14, 15]. CBD may also suppress inflammatory responses by reducing NF-κB and STAT1 activity, decreasing the production of pro-inflammatory cytokines such as TNF-α and IL-6, and inhibiting NLRP3 inflammasome activation [16, 17]. Nevertheless, CBD is highly lipophilic and exhibits poor aqueous solubility. Following oral administration, its bioavailability is very low (< 6%) because of extensive first-pass metabolism, which substantially limits its clinical application [18, 19]. Film-forming gels (FFGs) are an emerging topical drug-delivery platform that combines the drug-loading capacity of gels with the prolonged residence provided by an *in situ* formed film. In recent years, FFGs have shown particular promise for the transdermal delivery of poorly water-soluble compounds [20]. For lipophilic drugs such as CBD, the use of a polymeric matrix to modulate drug release and form a protective film on the skin may enhance local bioavailability [21]. After application, the resulting film reduces removal by clothing, prolongs residence time at the administration site, and promotes sustained drug release and penetration [22]. Transdermal delivery can also bypass hepatic first-pass metabolism, reduce systemic exposure, and increase drug concentrations at the target site [23, 24]. In addition, FFGs are easy to apply, generally biocompatible, and may improve patient comfort and adherence [25].

This study selected CBD as the active pharmaceutical ingredient, carboxymethyl cellulose sodium (CMC-Na) as the gel matrix, and polyvinylpyrrolidone (PVP) as the film-forming agent to construct a CBD film-forming gel. The formulation and preparation process were systematically optimized followed by comprehensive physicochemical characterization. Acute pain and inflammation models were then established in mice to evaluate the pharmacological performance of the CBD film-forming gel and explore its potential mechanisms of action. This study provided a theoretical and experimental basis for the development of a novel topical analgesic and anti-inflammatory formulation.

Materials and methods

Preparation of blank film-forming gel and single-factor screening

The blank film-forming gel was prepared using carboxymethyl cellulose sodium (CMC-Na) (Tianjin Kermel Chemical Reagent Co., Ltd., Tianjin, China) as the gel matrix, polyvinylpyrrolidone (PVP) (Hefei Basf Biotechnology Co., Ltd., Hefei, Anhui, China) as the film-forming agent, anhydrous ethanol as the film-promoting agent and co-solvent, and glycerol as the humectant. The effect of the amount of CMC-Na on gel quality was initially evaluated. Precisely weighed 0.1, 0.2, 0.3, 0.4 g of CMC-Na were added to 4.5 mL of distilled water and allowed to swell at room temperature for 12 h. Distilled water was then added to bring the final formulation weight to 10 g, and the mixtures were stirred until homogeneous. The resulting film-forming gels were comprehensively evaluated based on appearance, stability, viscosity, fineness, and film-forming capacity with each parameter being scored on a 10-point scale base, giving a maximum total score of 50 (Table 1). After the appropriate amount of CMC-Na had been identified, its amount was fixed at 0.2 g, and the effects of PVP, anhydrous ethanol, and glycerol on blank gel quality were systematically

Table 1. Quality evaluation criteria for film-forming gels.

Evaluation parameter	Unsatisfactory (1 - 2)	Acceptable (3 - 4)	Good (5 - 7)	Excellent (8 - 10)
Appearance	Poor color, aggregation	Discolored, slight liquefaction	Slightly discolored, adequately uniform	Appropriate color, translucent
Stability	Complete phase separation	Precipitation observed	No obvious stratification	Homogeneous distribution
Viscosity	Non-viscous or liquefied	Poor viscosity or slight liquefaction	Suboptimal viscosity	Appropriate viscosity
Fineness	Coarse texture	Slightly coarse	Relatively fine	Fine texture
Film-forming	Difficult to spread	Slightly uniform	Relatively uniform	Uniform, intact film

investigated. The amounts of PVP tested were 0.05, 0.15, 0.30, and 0.45 g, while the volumes of anhydrous ethanol were 1.5, 2.0, 2.5, and 3.0 mL, and the amounts of glycerol were 0.5, 1.0, and 1.5 g. During optimization, only one factor was varied at a time, while all other conditions were kept constant. All formulations were assessed using the same scoring criteria.

Orthogonal optimization of blank film-forming gel

Based on the results of the single-factor experiments, CMC-Na (factor A), PVP (factor B), and anhydrous ethanol (factor C) were selected as the principal formulation factors. An L9 (3^4) orthogonal array design was used to optimize the blank gel formulation with the comprehensive score as the response variable. Range analysis was performed to compare the relative influence of each factor on gel quality and to identify the optimal formulation.

Preparation of CBD-loaded film-forming gel and drug loading optimization

CBD (purity > 98%) (Heilongjiang Zhongsheng Biotechnology Co., Ltd., Jiamusi, Heilongjiang, China) was incorporated into the optimized blank gel matrix at amounts of 0.0007, 0.0013, 0.0019, and 0.0025 g. Each formulation was mixed thoroughly, and distilled water was added to bring the final weight to 10 g. The resulting CBD-loaded film-forming gels were evaluated according to the same criteria. The optimal CBD loading was selected by considering the formulation quality, the murine dosing ranges reported in the literature, and the administration area used in the present study.

Physicochemical characterization of CBD film-forming gel

The optimized CBD film-forming gel was subjected to physicochemical characterization. Color, homogeneity, visible aggregation, and spread ability were assessed by visual inspection. An appropriate amount of gel was applied uniformly to a flat surface, and the film-formation time was recorded. The integrity and flexibility of the resulting film were subsequently evaluated. The pH was measured using a PHS-3C pH meter (Shanghai LeiCi Instrument Co., Ltd., Shanghai, China), and particle size was determined using a BT-90 particle size analyzer (Dandong Bettersize Instruments Co., Ltd., Dandong, Liaoning, China). Physical stability was evaluated under elevated-temperature of 40 ± 2°C, low-temperature of 4 ± 2°C, and high-humidity of 75 ± 5%. The formulations were monitored for phase separation, precipitation, discoloration, and other visible physical changes.

Pharmacodynamic and safety evaluations

1. Experimental animals, grouping, and administration

Forty (40) healthy KM mice were obtained from the Animal Experiment Center of Jiamusi University (Jiamusi, Heilongjiang, China). The animals were maintained at 24 ± 2°C and 40 - 70% relative humidity with *ad libitum* access to standard chow and water. All animal procedures were performed in accordance with institutional

ethical guidelines and were approved by the Experimental Animal Ethics Committee of Jiamusi University (Jiamusi, Heilongjiang, China). The mice were randomly assigned to five groups with 8 animals per group including a control group receiving blank gel vehicle, a positive control group receiving 5 mg/g diclofenac diethylamine emulgel (Novartis Pharma AG, Basel, Switzerland), and low-, medium-, and high-dose CBD film-forming gel groups receiving 3.5, 5.0, and 6.5 mg/kg, respectively. One day before treatment, the dorsal and abdominal fur was removed to produce a depilated area of approximately 2 cm × 3 cm. The formulations were applied topically three times daily at 08:00, 13:00, and 18:00 for 14 consecutive days. Pharmacodynamic assessments were initiated 1 h after the final administration.

2. Acetic acid-induced writhing test

Analgesic activity was evaluated using the acetic acid-induced writhing model. One hour after the final administration, mice received an intraperitoneal injection of 0.6% acetic acid. Writhing responses were recorded during the 0 - 15, 15 - 30, and 30 - 45 min intervals after injection. The pain inhibition rate was calculated as follows.

Pain inhibition rate (%) = [(mean writhing count in the control group - mean writhing count in the treated group) / mean writhing count in the control group] × 100%

3. Xylene-induced ear edema assay

Acute local anti-inflammatory activity was assessed using the xylene-induced ear edema model. One hour after the final administration, 20 µL of xylene (Xilong Scientific Co., Ltd., Shantou, Guangdong, China) was applied uniformly to the inner and outer surfaces of the right auricle. One hour after xylene application, the mice were euthanized, and equal-diameter ear punches were collected from both ears and weighed. Ear swelling and the edema inhibition rate were calculated as follows.

Ear swelling (g) = weight of the right ear punch (g) - weight of the left ear punch (g)

Edema inhibition rate (%) = [(mean ear swelling in the control group - mean ear swelling in the treated group) / mean ear swelling in the control group] × 100%

4. Egg white-induced paw edema assay

Anti-inflammatory activity was further evaluated using the egg white-induced paw edema model. One hour after the final administration, 0.05 mL of fresh egg white was injected subcutaneously into the plantar surface of the right hind paw. Paw thickness was measured using digital calipers immediately before induction and at 1, 2, 3, and 4 h after induction. Paw edema and the swelling rate were calculated as follows.

Paw edema (mm) = postinduction paw thickness (mm) - preinduction paw thickness (mm)

Swelling rate (%) = [paw edema / preinduction paw thickness] × 100%

5. Histopathological examination

After completion of the paw edema assay, the mice were euthanized, and tissue from the inflamed region of the right hind paw was collected. Samples were fixed in 10% neutral buffered formalin, dehydrated through a graded ethanol series, embedded in paraffin, sectioned at a thickness of 5 µm, and stained with hematoxylin and eosin (H&E). Histopathological changes were examined by light microscopy with particular attention to interstitial widening, edema, inflammatory cell infiltration, and local structural alterations. Paw tissue from one untreated healthy KM mouse was included solely as a normal histological reference and was not part of the formal experimental grouping or statistical analysis.

6. Enzyme-linked immunosorbent assay (ELISA) quantification of serum inflammatory cytokines

After the pharmacodynamic assessments, orbital blood samples were collected from each mouse and centrifuged to obtain serum. Serum

concentrations of interleukin-4 (IL-4), interleukin-6 (IL-6), and tumor necrosis factor-α (TNF-α) were measured using commercial ELISA kits (Andy Gene Biotechnology Co., Ltd., Beijing, China) following manufacturer's instructions.

7. Preliminary safety assessment

Throughout the treatment and experimental periods, the general conditions of the mice including activity, food and water intake, and body weight were monitored and recorded. At the end of the study, the mice were euthanized, and the heart, liver, spleen, lungs, and kidneys were excised, weighed, and visually examined. Organ indices were calculated as follows.

Organ index (%) = (organ weight / body weight) × 100%

Statistical analysis

All statistical analyses were performed using SPSS version 27.0 (IBM Corp., Armonk, NY, USA). Data were presented as the mean ± standard deviation (mean ± SD). Comparisons between two groups were performed using Student's t-test. For comparisons among multiple groups at a single time point, one-way analysis of variance (ANOVA) followed by Dunnett's multiple-comparisons test was used. Time-course paw thickness and swelling-rate data were analyzed using two-way ANOVA followed by Dunnett's multiple-comparisons test to compare each treatment group with the control group at each time point. *P* value less than 0.05 was considered statistically significant.

Results

Optimization of blank film-forming gel formulation

The single-factor experiments demonstrated that 0.2 g CMC-Na produced the highest comprehensive score of 31, whereas 0.1, 0.3, and 0.4 g yielded scores of 27, 17, and 12, respectively. Gel viscosity increased progressively with increasing CMC-Na content. At lower amounts, the formulations exhibited insufficient viscosity and poor film-forming properties, whereas excessive CMC-Na produced overly viscous gels that were difficult to spread uniformly and prone to air-bubble entrapment, thereby compromising their appearance and usability. These findings indicated that 0.2 g CMC-Na provided the most appropriate balance between viscosity and film-forming capacity. The highest comprehensive score of PVP was 37 obtained at 0.30 g compared with scores of 35, 34, and 34 at 0.05, 0.15, and 0.45 g, respectively. Insufficient PVP resulted in films with inadequate mechanical strength and poor integrity, whereas increasing the PVP amount beyond 0.30 g did not further improve film-forming performance, despite maintaining acceptable appearance and stability. Therefore, 0.30 g PVP was considered optimal for producing a uniform and intact film. Increasing the amount of anhydrous ethanol progressively improved film formation. The highest score of 40 was obtained at 3.0 mL, whereas 1.5, 2.0, 2.5 mL yielded scores of 29, 34, 37, respectively, suggesting that 3.0 mL anhydrous ethanol was most favorable for film formation and overall formulation quality. For glycerol, 0.5 g produced the highest score of 40, while 1.0 and 1.5 g yielded scores of 37 and 31, respectively. These results suggested that an appropriate amount of glycerol improved film characteristics, whereas excessive glycerol might adversely affect film formation and overall formulation quality. Based on the single-factor screening results, an orthogonal experimental design was subsequently used to optimize the blank film-forming gel formulation, with CMC-Na, PVP, and anhydrous ethanol selected as the principal factors. Range analysis showed that the relative influence of these factors followed the order of CMC-Na (R = 8.67) > anhydrous ethanol (R = 2.00) > PVP (R = 1.33). Among them, the amount of CMC-Na had a statistically significant effect on the comprehensive formulation score ($P < 0.05$). The optimal combination was identified as 0.2 g of CMC-Na, 0.3 g of PVP, and 3.0 mL of anhydrous ethanol. This formulation was consistent with the trends observed in the single factor experiments and was therefore selected as the blank gel matrix for subsequent

preparation of the CBD-loaded film-forming gel.

Determination of CBD loading and physicochemical characterization of CBD film-forming gel

Based on the optimized blank gel matrix, the effects of different CBD loadings on formulation quality were systematically evaluated. CBD loadings of 0.0007, 0.0013, and 0.0019 g per 10 g of gel yielded comprehensive scores of 39, 38, and 38, respectively. When the CBD content was increased to 0.0025 g, the total score decreased to 36, primarily because of darkening of the formulation. Considering both the formulation quality and the CBD dose range reported in mice, 0.0019 g of CBD per 10 g of gel was selected as the optimal loading. The final optimized formulation consisted of 0.0019 g of CBD, 0.2 g of CMC-Na, 0.3 g of PVP, 0.5 g of glycerol, and 3.0 mL of anhydrous ethanol with distilled water added to a final weight of 10 g. Physicochemical characterization showed that the optimized CBD film-forming gel was pale milky-white and translucent with a fine and homogeneous texture, no visible aggregation, and good spread ability. Following topical application, the formulation formed a uniform, flexible, and transparent film within 2 – 3 min with satisfactory integrity and permeability. The pH ranged from 5.5 to 6.0, which was close to the physiological pH of the human skin surface and suggested a low potential for skin irritation. Particle-size analysis showed a mean diameter of 12.4 μm. Stability testing under elevated-temperature, low-temperature, and high-humidity conditions revealed no visible phase separation, precipitation, discoloration, or other marked changes in appearance, indicating favorable physical stability. Overall, the optimized CBD film-forming gel had a clearly defined composition, satisfactory physicochemical characteristics, and favorable stability, thereby providing an appropriate formulation basis for subsequent pharmacodynamic evaluation.

Analgesic activity of CBD film-forming gel

The analgesic activity of the CBD film-forming gel was evaluated using the acetic acid-induced writhing model, and the results showed that the number of writhing responses recorded at 15, 30, and 45 min after acetic acid injection. Compared with the control group, all treatment groups exhibited varying degrees of reduction in writhing responses with the most pronounced effect observed in the high-dose group. At 15 min, the high-dose group showed 27.5 ± 2.9 writhing responses, which was significantly lower than the 45.0 ± 4.3 responses observed in the control group. At 30 min, the number of writhing responses in the high-dose group decreased further to 19.9 ± 1.6, compared with 23.3 ± 2.6 in the positive control group and 23.1 ± 2.9 in the medium-dose group. At 45 min, the high-dose group exhibited 5.6 ± 0.6 writhing responses, which was significantly lower than that of the positive control group (9.0 ± 0.8) ($P < 0.05$) (Figure 1). The pain inhibition rates demonstrated that the low-dose group exhibited relatively modest analgesic activity, whereas the medium-dose group produced effects comparable to those of the positive control group at 30 and 45 min. The high-dose group consistently showed the greatest reduction in writhing responses across all observation periods. The calculated pain inhibition rate reached 60.0% in the high-dose group, compared with 35.7% in the positive control group (Figure 2). These findings indicated that the CBD film-forming gel reduced acetic acid-induced nociceptive responses in mice and exhibited an apparent dose-dependent analgesic effect with the high-dose formulation showing the greatest efficacy.

Inhibitory effects of CBD film-forming gel on xylene-induced ear edema

The anti-inflammatory activity of the CBD film-forming gel against acute local inflammation was evaluated using the xylene-induced ear edema model. The results showed that the weights of the xylene-treated ear punches were higher than those of the corresponding untreated ear punches in all groups, confirming the successful induction of ear edema. Ear swelling, calculated as the difference between the weights of the xylene-treated and untreated ear punches, was

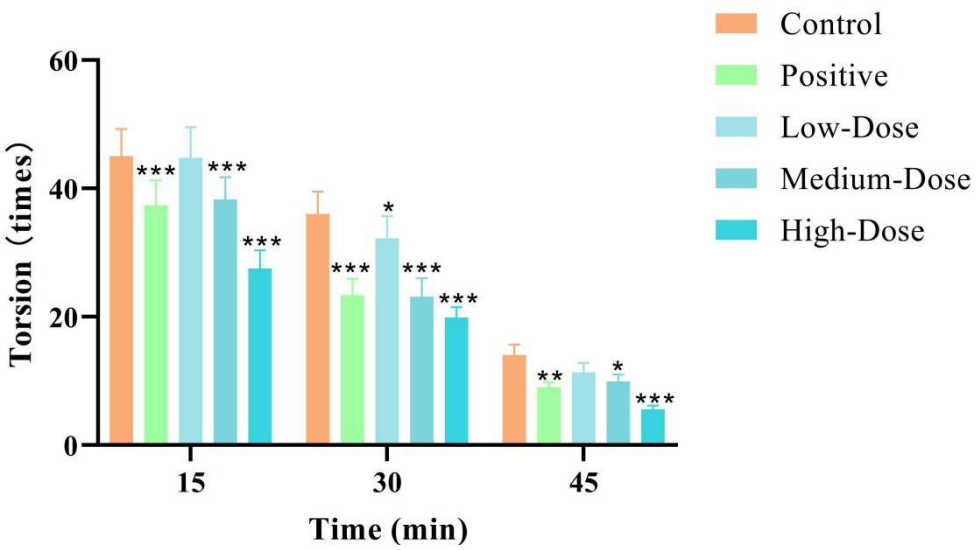

Figure 1. Analgesic effects of CBD film-forming gel in acetic acid-induced writhing test. *: $P < 0.05$, **: $P < 0.01$, ***: $P < 0.001$ compared with the control group.

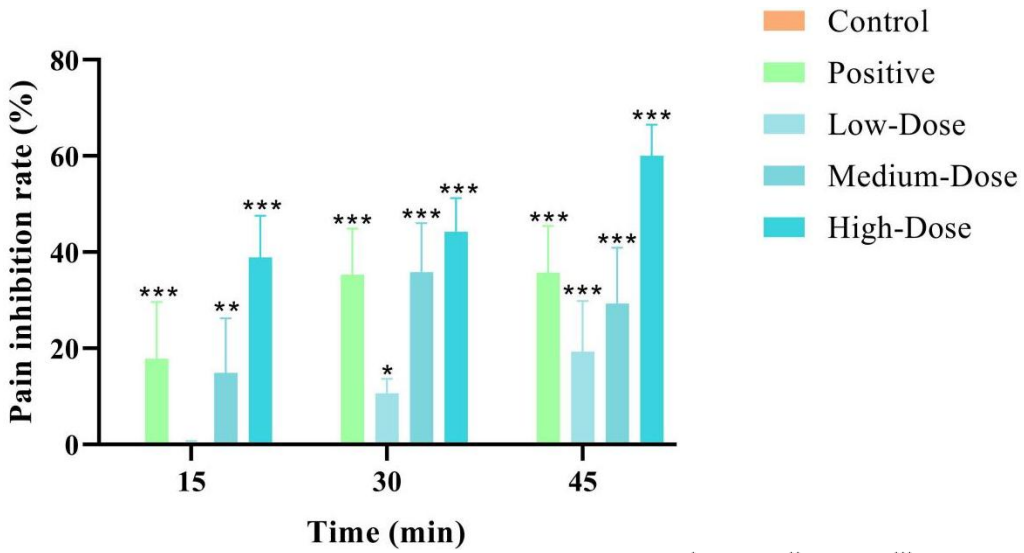

Figure 2. Pain inhibition rates of CBD film-forming gel in the mouse acetic acid writhing test. *: $P < 0.05$, **: $P < 0.01$, ***: $P < 0.001$ compared with the control group.

0.110, 0.078, 0.097, 0.081, and 0.041 g in control, positive control, low-dose, medium-dose, and high-dose groups, respectively. Compared with the control group, all treatment groups exhibited varying degrees of reduction in ear swelling, with the greatest reduction observed in the high-dose group (Figures 3). The corresponding ear swelling inhibition rates were 29.55%, 12.37%, 26.12%, and 62.54% in the positive control, low-dose, medium-dose, and high-dose groups, respectively. The inhibitory effect observed in the medium-dose group was comparable to that of the positive control group, whereas the high-dose group showed the highest inhibition rate (Figure 4). These findings indicated that the CBD film-forming gel attenuated xylene-induced acute ear edema in mice with a generally dose-dependent pattern and the most pronounced effect observed at the high dose.

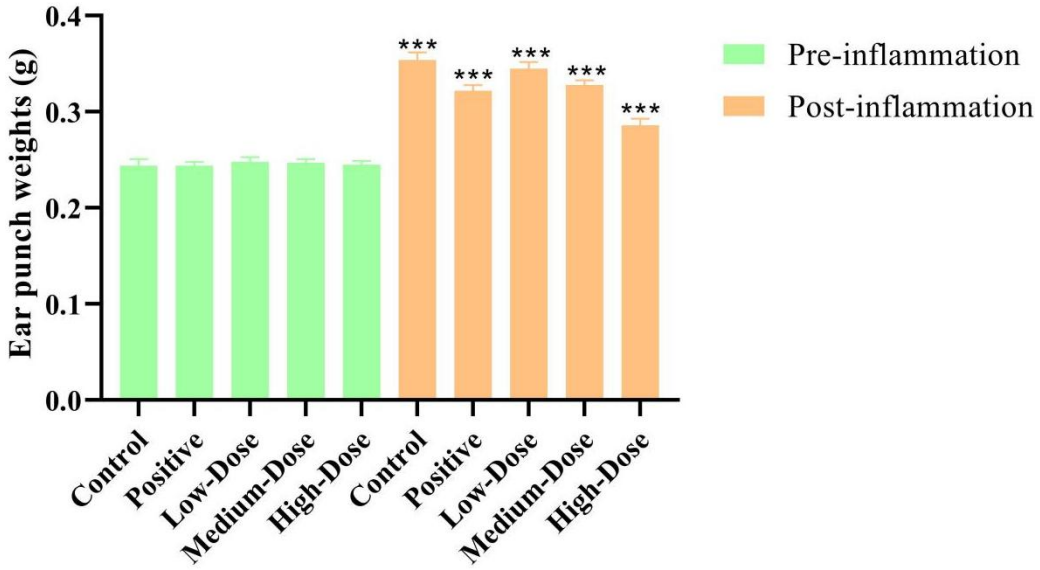

Figure 3. Ear punch weights before and after xylene induction. ***: $P < 0.001$ compared with the Pre-inflammation group.

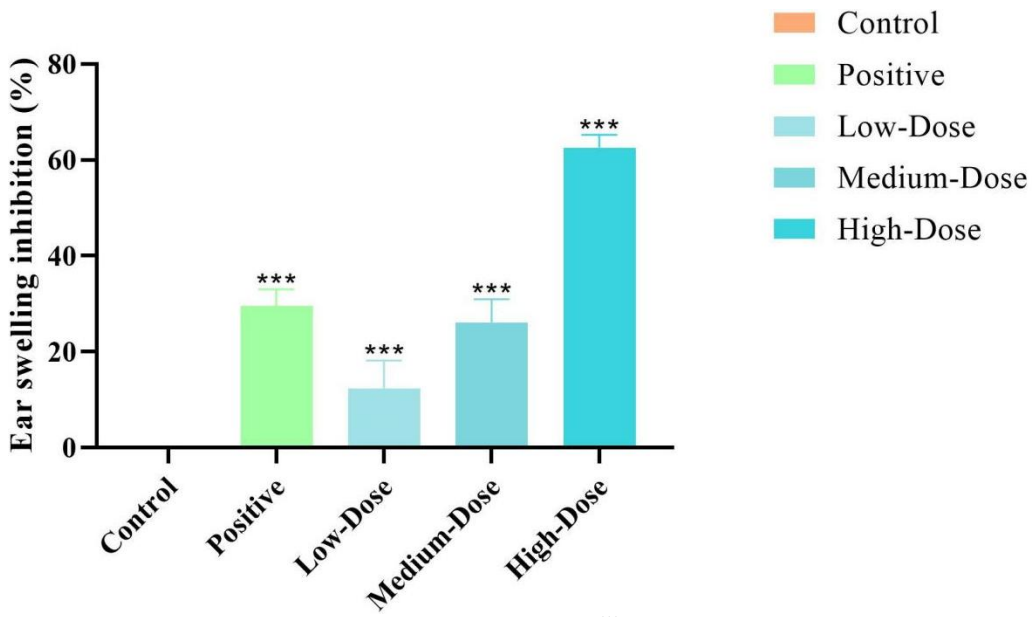

Figure 4. Inhibition rate of ear swelling in mice treated with CBD film-forming gel. ***: $P < 0.001$ compared with the control group.

Effects of CBD film-forming gel on egg white-induced paw edema and histopathological alterations

The anti-inflammatory activity of the CBD film-forming gel was further evaluated using an egg white-induced paw edema model. The results showed that the paw thickness increased in all groups after induction compared with baseline, confirming the successful establishment of the inflammatory model. Compared with the control group, the positive control and the medium- and high-dose CBD film-forming gel groups generally exhibited lower mean paw thickness values after induction, whereas the low-dose group showed a relatively modest response. Paw thickness increased markedly in all groups at 1 h and continued to rise in the control group, reaching its highest level at 3 h. The medium- and high-

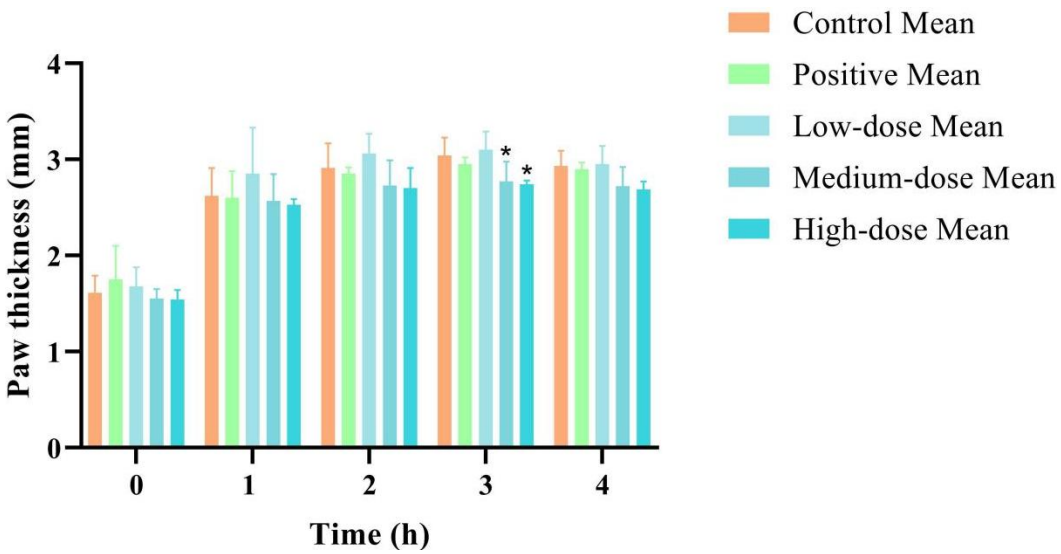

Table 5. Paw thickness measurements across experimental groups. *: $P < 0.05$ compared with the control group.

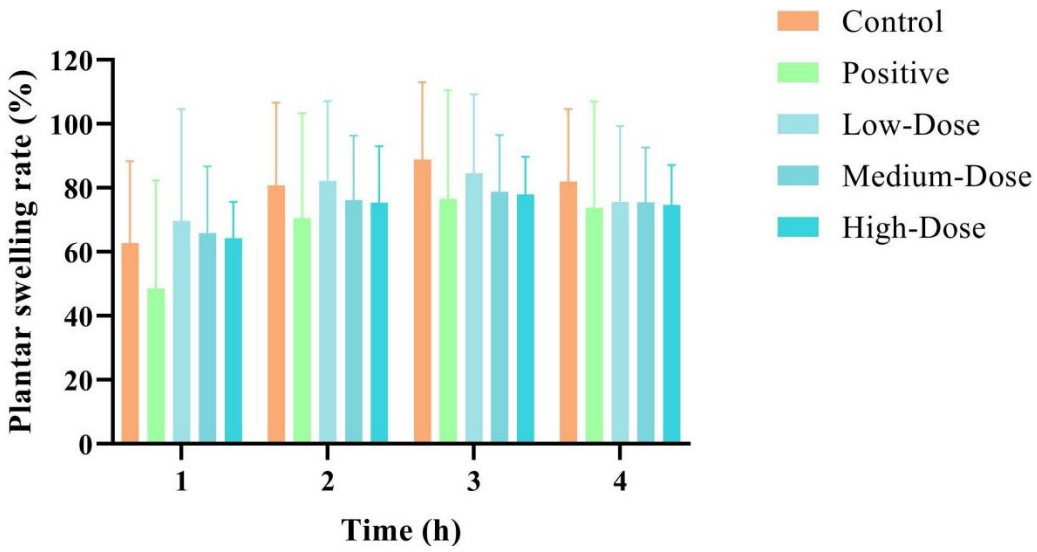

Figure 6. Foot swelling rates in each group of mice.

dose groups showed lower mean paw thickness values than the control group at 2 – 4 h. At 4 h, paw thickness was 2.72 ± 0.20 mm in the medium-dose group and 2.69 ± 0.08 mm in the high-dose group, compared with 2.93 ± 0.16 mm in the control group and 2.90 ± 0.07 mm in the positive control group (Figures 5). The paw swelling rates showed that, although the medium- and high-dose groups exhibited numerical reductions in paw swelling, the differences between the treatment groups and the control group did not reach statistical significance at any time point (Figure 6). These findings suggested that the CBD film-forming gel showed a tendency to alleviate egg white-induced acute paw edema, particularly at the medium and high doses, although this effect required further confirmation. Histopathological examination demonstrated that paw tissue from the untreated healthy mouse exhibited intact tissue architecture, a continuous epidermis, and clearly defined dermal and subdermal layers

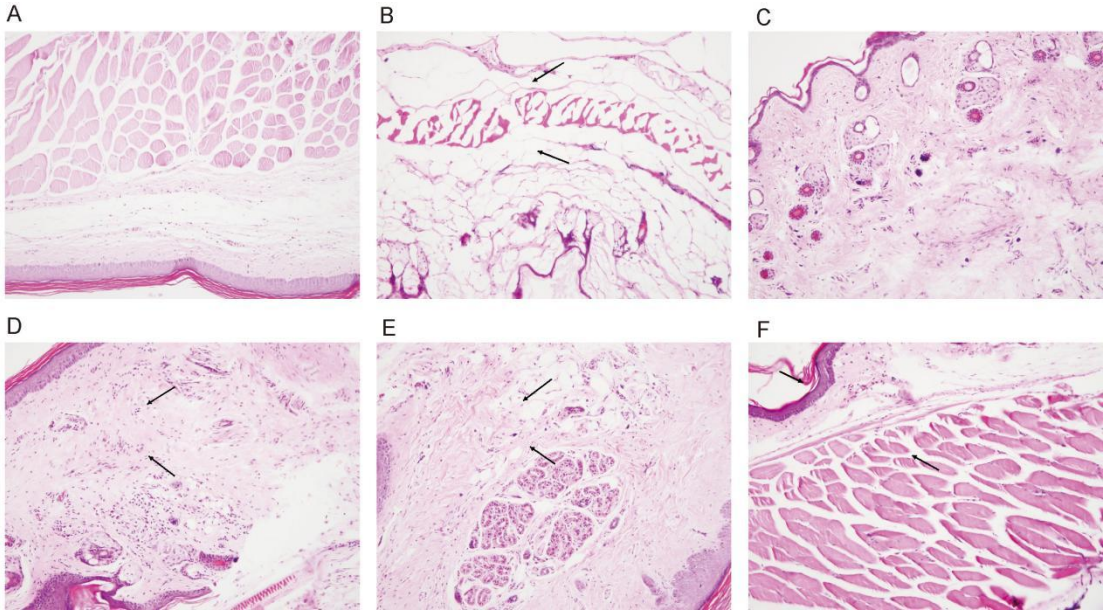

Figure 7. Histopathological changes in paw tissues from mice in each group (HE stain, 200×). **A.** Normal group (healthy mice without any treatment as baseline reference). **B.** Control group (model group with acetic acid-induced inflammation without treatment). **C.** Positive control group. **D.** Low-dose group. **E.** Medium-dose group. **F.** High-dose group. The black arrows indicated widened interstitial spaces, edema, and inflammatory cell infiltration.

without evident edema or inflammatory cell infiltration. In contrast, the control group showed marked histopathological alterations including widened interstitial spaces, tissue edema, and inflammatory cell infiltration. Compared with the control group, the positive control and CBD film-forming gel-treated groups exhibited varying degrees of histopathological improvement. These changes were more pronounced in the medium- and high-dose groups as evidenced by reduced interstitial widening, alleviated edema, decreased inflammatory cell infiltration, and partial restoration of tissue architecture. The low-dose group also showed modest improvement, although the extent of recovery was relatively limited (Figure 7). These histopathological findings were generally consistent with the trend observed in the paw edema measurements and suggested that the CBD film-forming gel might alleviate local inflammatory tissue injury.

Effects of CBD film-forming gel on serum inflammatory cytokine levels

The results of serum concentrations of IL-4, IL-6, and TNF-α showed that treatment with the CBD film-forming gel produced varying changes in circulating inflammatory cytokine levels compared with the control group. The serum IL-4, IL-6, and TNF-α concentrations In the control group were 107.5 ± 6.7, 2.555 ± 0.37, and 479.9 ± 112 pg/mL, respectively, while the corresponding values were 127.5 ± 7.6, 2.352 ± 0.27, and 423.8 ± 84 pg/mL in the high-dose group, respectively. Notably, serum IL-4 levels were significantly higher in the high-dose group than in the control group ($P < 0.001$). In contrast, IL-6 and TNF-α levels showed numerical decreases in the high-dose group, although these differences did not reach statistical significance. Similar patterns were observed in the positive control and medium-dose groups, whereas the low-dose group showed comparatively modest changes (Figure 8). These findings suggested that the CBD film-forming gel might modulate systemic inflammatory cytokine profiles under the present experimental conditions. In particular, the marked increase in IL-4 in the high-dose group, together with the downward trends

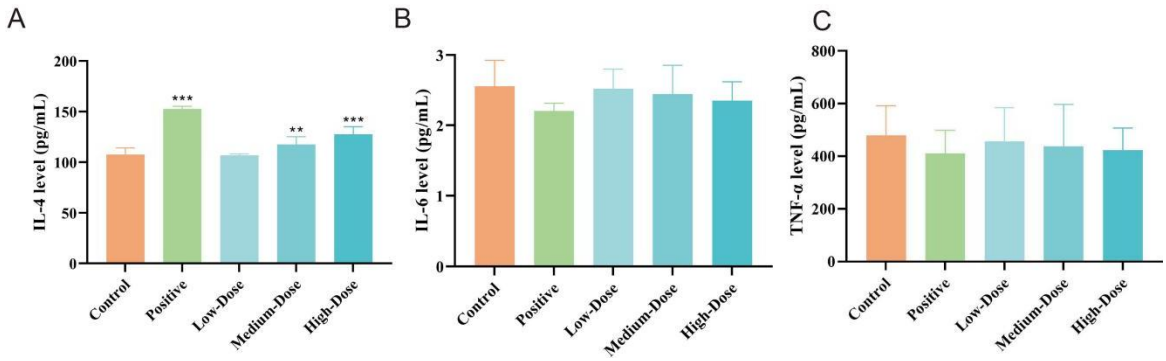

Figure 8. The levels of IL-4 (**A**), IL-6 (**B**), and TNF-α (**C**) in mice from each group. **: $P < 0.01$, ***: $P < 0.001$ compared with the control group.

in IL-6 and TNF-α, indicated a potential immunomodulatory effect. However, further studies were required to confirm the underlying mechanisms.

Preliminary safety evaluation of CBD film-forming gel

Throughout the experimental period, mice in all groups generally maintained normal food intake and activity levels, and body weight increased progressively without significant differences among groups. These observations suggested that the CBD film-forming gel did not adversely affect the general health status of the animals under the present experimental conditions. Analysis of major organ indices showed no significant abnormalities in the heart, liver, spleen, lung, or kidney indices of mice treated with low, medium, or high doses of the CBD film-forming gel compared with the control group, indicating no detectable treatment-related organ toxicity. In contrast, the positive control group showed higher liver and spleen indices than the control group. In addition, occasional lethargy, somnolence, and reduced food intake were observed in some animals in the positive control group during the experimental period. Overall, no overt signs of toxicity were observed following treatment with the CBD film-forming gel, supporting a favorable preliminary safety profile under the conditions of this study.

Discussion

CBD has considerable potential as an analgesic and anti-inflammatory agent. However, its poor aqueous solubility, high lipophilicity, and low oral bioavailability present substantial formulation challenges [26, 27]. To address these limitations, the present study employed film-forming gel technology as a topical delivery strategy. Through systematic optimization of both the blank matrix and the CBD-loaded formulation, a physically stable gel with satisfactory film-forming properties was obtained. Physicochemical characterization confirmed that the optimized formulation was homogeneous, had a skin-compatible pH and appropriate particle size, and remained stable under different storage conditions. These findings indicated that the formulation met the basic quality requirements for topical administration and provided a suitable basis for subsequent pharmacodynamic evaluation. The CBD film-forming gel demonstrated marked analgesic activity and potential local anti-inflammatory effects across several experimental animal models. In the acetic acid-induced writhing test, the high-dose formulation significantly reduced the number of writhing responses and achieved a pain inhibition rate of 60.0%, indicating a substantial effect on acute inflammatory pain. In the xylene-induced ear edema animal model group, the formulation reduced ear swelling in a generally dose-dependent manner with the greatest inhibition observed in the high-dose group. In the egg white-induced paw edema model, the medium- and high-dose groups showed lower mean paw

thickness and swelling rates than the control group at later time points. However, these differences did not reach statistical significance. Therefore, the paw edema findings should be interpreted as indicating an improvement trend rather than definitive evidence of anti-inflammatory efficacy. Taken together, the results suggested that topical CBD delivery might alleviate inflammatory pain and suppress acute local inflammatory responses, although the magnitude of the effect varied among experimental models. Histopathological findings provided additional support for the local effects of the formulation. H&E staining revealed reduced tissue edema, interstitial widening, and inflammatory cell infiltration in the CBD-treated groups, particularly in the medium- and high-dose groups. These morphological improvements were generally consistent with the downward trend observed in paw swelling. The ELISA analysis further showed alterations in serum IL-4, IL-6, and TNF-α levels in the medium- and high-dose groups. Notably, serum IL-4 levels were significantly higher in the high-dose group than in the control group ($P < 0.001$), whereas IL-6 and TNF-α levels showed numerical decreases that did not reach statistical significance. These findings suggested that the CBD film-forming gel might exert a modest immunomodulatory effect on systemic inflammatory mediator profiles. However, the cytokine data should be regarded as supportive evidence of anti-inflammatory activity rather than definitive proof of involvement of a specific molecular pathway. Previous studies have suggested that CBD may exert anti-inflammatory effects through modulation of CB2 receptor-related and NF-κB signaling pathways [28, 29]. Because these pathways were not directly examined in the present study, mechanistic interpretations should remain cautious. The current findings also raised the possibility that prolonged residence on the skin and gradual local permeation contributed to the pharmacological effects of the CBD film-forming gel. However, dedicated transdermal permeation and mechanistic studies are required to confirm this hypothesis. Preliminary safety evaluation showed that mice treated with the CBD film-forming gel maintained generally normal activity, food intake, and body weight gain with no significant abnormalities in major-organ indices. These observations suggested that the formulation was well tolerated under the conditions tested. In contrast, the positive control group showed increased liver and spleen indices and occasional behavioral abnormalities, although these findings required further confirmation. Overall, the CBD film-forming gel exhibited favorable physicochemical properties, marked analgesic activity, potential local anti-inflammatory effects, and an acceptable preliminary safety profile. However, the present study was limited to formulation optimization and initial pharmacodynamic assessment. Future studies should investigate transdermal permeation, *in vitro* and *in vivo* drug-release behavior, pharmacokinetics, long-term safety, and the molecular mechanisms underlying its analgesic and anti-inflammatory effects. These investigations will be essential to determine the translational potential of the formulation as a topical therapeutic agent.

Acknowledgements

This research was supported by Basic Scientific Research Project for Heilongjiang Provincial Colleges and Universities (Grant No. 2021-KYYWF-0587).

References

1. Lou Z, Bu F. 2025. Recent advances in osteoarthritis research: A review of treatment strategies, mechanistic insights, and acupuncture. Medicine (Baltimore). 104(4):e41335.
2. Zhang X, Li X, Jiang T, Fu J. 2026. A brief review of Chikungunya fever: From molecular virology to countermeasures. Infect Med. 5(1):100231.
3. Rometsch C, Martin A, Junne F, Cosci F. 2025. Chronic pain in European adult populations: A systematic review of prevalence and associated clinical features. Pain. 166(4):719–731.
4. Zhu M, Zhang J, Liang D, Qiu J, Fu Y, Zeng Z, *et al*. 2025. Global and regional trends and projections of chronic pain from 1990 to 2035: Analyses based on global burden of diseases study 2019. Br J Pain. 19(2):125–137.

5. Amaechi O, Huffman MM, Featherstone K. 2021. Pharmacologic therapy for acute pain. Am Fam Physician. 104(1):63–72.
6. Wang J, Doan LV. 2024. Clinical pain management: Current practice and recent innovations in research. Cell Rep Med. 5(10):101786.
7. Wirth T, Lafforgue P, Pham T. 2024. NSAID: Current limits to prescription. Joint Bone Spine. 91(4):105685.
8. Bindu S, Mazumder S, Bandyopadhyay U. 2020. Non-steroidal anti-inflammatory drugs (NSAIDs) and organ damage: A current perspective. Biochem Pharmacol. 180:114147.
9. Nadeau SE, Wu JK, Lawhern RA. 2021. Opioids and chronic pain: An analytic review of the clinical evidence. Front Pain Res. 17(2):721357.
10. Volkow ND, Blanco C. 2021. The changing opioid crisis: Development, challenges and opportunities. Mol Psychiatry. 26(1):218–233.
11. Tihăuan BM, Onisei T, Slootweg W, Gună D, Iliescu C, Chifiriuc MC. 2025. Cannabidiol—A friend or a foe? Eur J Pharm Sci. 208:107036.
12. Martinez Naya N, Kelly J, Corna G, Golino M, Abbate A, Toldo S, *et al*. 2023. Molecular and cellular mechanisms of action of cannabidiol. Molecules. 28(16):5980.
13. Binkowska AA, Jakubowska N, Redeł A, Laskowska S, Szlufik S, Brzezicka A. 2024. Cannabidiol usage, efficacy, and side effects: Analyzing the impact of health conditions, medications, and cannabis use in a cross-sectional online pilot study. Front Psychiatry. 15:1356009.
14. Alexander C, Jeon J, Nickerson K, Hassler S, Vasefi M. 2025. CBD and the 5-HT1A receptor: A medicinal and pharmacological review. Biochem Pharmacol. 233:116742.
15. Wang W, Xie G, Xu B, Xie J, Cao D, Song X, *et al*. 2026. Effects and mechanisms of cannabidiol in attenuating orofacial inflammatory pain and ameliorating pain-related affective deficits. Brain Res Bull. 237:111813.
16. Suryavanshi SV, Zaiachuk M, Pryimak N, Kovalchuk I, Kovalchuk O. 2022. Cannabinoids alleviate the LPS-induced cytokine storm *via* attenuating NLRP3 inflammasome signaling and TYK2-mediated STAT3 signaling pathways *in vitro*. Cells. 11(9):1391.
17. Yndart Arias A, Kolishetti N, Vashist A, Madepalli L, Llaguno L, Nair M. 2023. Anti-inflammatory effects of CBD in human microglial cell line infected with HIV-1. Sci Rep. 13(1):7376.
18. Paczkowska-Walendowska M, Trzaskoma P, Dziopa A, Moeini A, Soczawa M, Krasiński Z, *et al*. 2025. Innovative strategies to enhance the bioavailability of cannabidiol: Nanotechnology and advanced delivery systems. Pharmaceuticals. 18(11):1637.
19. Na JH, Lee YM. 2025. Pharmacological and pharmacokinetic profile of cannabidiol in human epilepsy: A review of metabolism, therapeutic drug monitoring, and interactions with antiseizure medications. Biomolecules. 15(12):1668.
20. Pünnel LC, Lunter DJ. 2021. Film-forming systems for dermal drug delivery. Pharmaceutics. 13(7):932.
21. Lefebvre È, Tawil N, Yahia LH. 2024. Transdermal delivery of cannabidiol for the management of acute inflammatory pain: A comprehensive review of the literature. Int J Mol Sci. 25(11):5858.
22. Touitou E, Natsheh H, Zailer J. 2023. Film forming systems for delivery of active molecules into and across the skin. Pharmaceutics. 15(2):397.
23. Jain M, Hudson R, Tarrell A, Green DJ, Clifford JJ, Watt K, *et al*. 2026. Results of an exploratory crossover pharmacokinetic study evaluating a natural hemp extract-based cosmetic product: Comparison of topical and oral routes of administration. Pharmaceuticals. 19(2):231.
24. Kushwaha R, Palei NN. 2024. Transdermal drug delivery systems: Different generations and dermatokinetic assessment of drug concentration in skin. Pharm Med. 38(6):407–427.
25. Milinković S, Đekić L. 2025. Film-forming solutions for cutaneous application: Current challenges and future directions in formulation design and characterization framework. J Drug Deliv Sci Technol. 108:106863.
26. Fraguas-Sánchez AI, Fernández-Carballido A, Martin-Sabroso C, Torres-Suárez AI. 2020. Stability characteristics of cannabidiol for the design of pharmacological, biochemical and pharmaceutical studies. J Chromatogr B. 1150:122188.
27. Rusu A, Farcaș A-M, Oancea O-L, Tanase C. 2025. Cannabidiol in skin health: A comprehensive review of topical applications in dermatology and cosmetic science. Biomolecules. 15(9):1219.
28. Jiang Z, Jin S, Fan X, Cao K, Liu Y, Wang X, *et al*. 2022. Cannabidiol inhibits inflammation induced by *Cutibacterium acnes*-derived extracellular vesicles *via* activation of CB2 receptor in keratinocytes. J Inflamm Res. 15:4573–4583.
29. Kuzumi A, Yoshizaki-Ogawa A, Fukasawa T, Sato S, Yoshizaki A. 2024. The potential role of cannabidiol in cosmetic dermatology: A literature review. Am J Clin Dermatol. 25(6):951–966.